Karaelmas Science and Engineering Journal
Journal home page: https://dergipark.org.tr/tr/pub/karaelmasfen
DOI: 10.7212/karaelmasfen.1796249

Research Article
Received / Geliş tarihi : 03.10.2025
Accepted / Kabul tarihi : 20.11.2025

Graph Theory Metrics-based Functional Brain Network Analysis in Dyslexia

Disleksi'de Graf Teorisi Metriklerine Dayalı Fonksiyonel Beyin Ağı Analizi

Ozlem Karabiber Cura[1]*, Sevde Dervisoglu[1], Gunet Eroglu[2]

[1]Izmir Katip Celebi University, Department of Biomedical Engineering, Izmir, Türkiye
[2]Bahçeşehir University, Department of Computer Engineering, Istanbul, Türkiye

Abstract

Developmental dyslexia, a neurodevelopmental disorder affecting 5-10% of school-aged children, involves persistent reading, decoding, and spelling difficulties. Electroencephalography (EEG), especially when combined with graph theory, offers a powerful, non-invasive method for exploring the neural basis of dyslexia. This study examines neuroplastic changes in 14 subjects with dyslexia during a 60-day cognitive training protocol, utilizing EEG-based functional connectivity and brain network analysis. The international 10–20 system is used to capture EEG signals from 14 scalp locations that encompass the frontal, temporal, parietal, and occipital lobes. The EEG recordings from Days 1 and 60 are used to extract a variety of connectivity metrics, including correlation coefficients, covariances, cross-power spectral densities, magnitude-squared coherence, and entropy-based metrics. Additionally, seven graph theory metrics (assortativity, transitivity, clustering coefficient, global efficiency, local efficiency, modularity, and characteristic path length) are calculated using connectivity measures to assess changes in large-scale brain networks. In order to evaluate the impact of cognitive training, EEG-derived features are classified using machine learning models such as logistic regression, decision trees, bagging trees, k-nearest neighbor, and support vector machines. By Day 60, graph-based connectivity tests revealed enhanced long-range functional connectivity and better brain network integration. These results imply that children with dyslexia may have quantifiable neuroplasticity as a result of cognitive instruction. EEG-based graph metrics are also highlighted in the paper as possible indicators for tracking dyslexic children's cognitive development and the effectiveness of their treatment.

Keywords: Brain network metrics, cognitive training, developmental dyslexia, EEG, functional connectivity, graph theory, machine learning.

Öz

Okul çağındaki çocukların %5-10'unu etkileyen nörogelişimsel bir bozukluk olan gelişimsel disleksi, okuma, kod çözme ve yazımda kalıcı zorluklarla karakterizedir. Elektroensefalografi (EEG), özellikle graf teori ile birleştirildiğinde, disleksinin nöral temelini keşfetmek için güçlü ve invaziv olmayan bir yöntem sunar. Bu çalışma, EEG tabanlı işlevsel bağlantı ve beyin ağı analizi kullanılarak 60 günlük bir bilişsel eğitim protokolü boyunca disleksili 14 denekte nöroplastik değişiklikleri araştırmaktadır. EEG sinyalleri, uluslararası 10-20 sistemini izleyerek frontal, temporal, parietal ve oksipital lobları kapsayan 14 kafa derisi bölgesinden kaydedilmiştir. 1. ve 60. günlere ait EEG kayıtları, korelasyon katsayısı, kovaryans, çapraz güç spektral yoğunluğu, büyüklük kareli koherans ve entropi tabanlı metrikler gibi çeşitli bağlantı metriklerini çıkarmak için kullanılmıştır. Ek olarak, büyük ölçekli beyin ağı değişikliklerini değerlendirmek için hesaplanan bağlantı ölçümleri kullanılarak yedi graf teori metriği (asortivite, geçişlilik, kümeleme katsayısı, küresel verimlilik, yerel verimlilik, modülerlik ve karakteristik yol uzunluğu) hesaplanmıştır. Bilişsel eğitimin etkisini değerlendirmek için, EEG'den türetilen özellikler lojistik regresyon, karar ağaçları, torbalama ağaçları, k-en yakın komşu ve destek vektör makineleri gibi makine

*Corresponding author: ozlem.karabiber@ikcu.edu.tr

Ozlem Karabiber Cura orcid.org/0000-0001-8650-1137
Sevde Dervisoglu orcid.org/0009-0004-6932-107X
Gunet Eroglu orcid.org/0000-0001-8382-8417

öğrenimi modelleri kullanılarak sınıflandırılmıştır. 60. güne gelindiğinde, grafik tabanlı bağlantı testleri, gelişmiş uzun menzilli işlevsel bağlantı ve daha iyi beyin ağı entegrasyonunu ortaya koymuştur. Bu bulgular, disleksili çocukların bilişsel eğitim sonucunda ölçülebilir nöroplastisiteye sahip olabileceğini göstermektedir. EEG tabanlı grafik metrikler de makalede; disleksili çocukların bilişsel gelişimlerini ve tedavilerinin etkinliğini izlemek için olası göstergeler olarak vurgulanmıştır.

Anahtar Kelimeler: Beyin ağı ölçümleri, bilişsel eğitim, EEG, fonksiyonel bağlantı, gelişimsel disleksi, graf teori, makine öğrenmesi.

1. Introduction

Developmental dyslexia is a common and heterogeneous neurodevelopmental disorder characterized by persistent difficulties in reading acquisition, decoding, and spelling, despite normal intelligence, adequate educational exposure, and intact sensory function (Peterson & Pennington, 2012). Families and school teachers are not very aware of dyslexia in society. Although the number of persons with dyslexia is believed to be at least 10% in every society, 41.600 out of 85 million people in Turkey have been diagnosed with the disorder, making up only 0.05% of the total population, according to the Turkish Dyslexia Association (Eroglu et al., 2022). Although traditionally viewed as a phonological processing disorder, growing evidence suggests that dyslexia stems from a more complex interplay of deficits in phonological awareness, working memory, attentional control, and executive functioning (Snowling & Hulme, 2012). These deficits indicate the involvement of multiple, distributed brain regions and network-level dysfunctions, rather than a single localized abnormality.

Teacher reports, observations, and standardized tests are used to diagnose dyslexia in youngsters. Frequent reading lag may be a sign of dyslexia; however, timing and criteria can differ, requiring further neuropsychological or medical testing (Castillo-Barnes et al., 2024). Electroencephalography (EEG) has emerged as a powerful, non-invasive, and cost-effective tool for investigating the temporal dynamics of brain function in neurodevelopmental disorders. Owing to its excellent temporal resolution, EEG is particularly suited for capturing the fast-paced neural processes involved in language and reading. In recent years, the focus of EEG analysis has shifted beyond traditional frequency and power domain measures, toward understanding functional connectivity—the statistical dependencies between activity recorded at different brain regions. This shift has enabled the application of graph theory, a mathematical framework that models the brain as a complex network, with nodes representing electrodes (or brain regions) and edges representing functional interactions such as coherence or correlation. Using this approach, researchers can quantify how efficiently the brain communicates, how specialized subnetworks interact, and how brain dynamics change in response to interventions. Cross-frequency coupling analysis is used in a study by Castillo-Barnes et al., (2024) to investigate dyslexia in Spanish readers. To measure and categorize activations, it makes use of CFS (Cross-Frequency phase Synchronization) maps and EEG signals. Potential implications in early dyslexic identification are suggested by the research findings, which demonstrate sensitivity to brain patterns associated with dyslexia. In another study, the characteristics triggered during the serial Rapid-Automatized Naming (RAN) task using electroencephalography and eye tracking, which may help distinguish between children with dyslexia and chronological age controls, are examined. Results under non-confounding and phonologically identical situations revealed substantial variations in fixation-related potentials amplitudes between the dyslexia and chronological age control groups. The average extracted component amplitude is a strong predictor of RAN performance, indicating a connection between dyslexia and neurocognitive processes during serial RAN (Christoforou et al., 2021). Through complicated network analysis of electroencephalography (EEG) data, a study investigates brain mechanisms involved in low-level auditory processing. Brain connectivity is inferred using Phase-Amplitude Coupling (PAC) between EEG electrodes, which allowed graphs to be created. The clustering coefficient, path length, and small-worldness—all graph theory metrics—are examined over time for both dyslexic and control patients. The results show that dyslexic individuals have changed network properties, namely a loss of small-world topology (Gallego-Molina et al., 2022). Another study examines the functional brain networks of dyslexic children during extended attention. The study included 15 kids with dyslexia and 15 kids without the disorder. The results showed omission and commission mistakes, lower efficiency and clustering coefficients, and significant variations in task metrics. The study's greatest classification accuracy of 96.7% is attained using a k-nearest neighbor classifier, indicating that dyslexic brain networks had poor functional segregation and disturbed information transfer (Seshadri et al., 2023). A Brain Comput-

er Interface Device and an Interactive Linguistic Software Tool are used in another study to categorize university students with dyslexia. The EEG signals of 14 normally developed individuals and 12 children with dyslexia are recorded. To find quantitative EEG variables that describe dyslexia in various brain regions, a Random Forests classifier is trained using spectral information. Results indicated that the entire brain had high accuracy, sensitivity, and specificity (above 95%), with the left and right hemispheres coming in second and third (Christodoulides et al., 2022). Through the use of evoked-related potentials during a Visual Continuous Performance Task, another study suggests an effective technique for dyslexia identification. The approach makes use of eight-fold cross-validation and five classifiers as part of ensemble learning classification approaches. The sensitivity and specificity reported in the study are 81.2% and 93.7%, respectively, while the overall average classification accuracy is 87.5% (Zaree et al., 2023). The Wavelet Scattering Transform (WST)-based dyslexia detection approach is proposed in another study. The WST approach outperformed three other approaches, with an average accuracy of 96.96% and 97.12% for datasets 1 and 2, respectively. The accuracy of WST features is further improved to 98.72% and 98.67% through the majority voting method (Parmar & Paunwala, 2023). Asynchrony in the EEG signals of dyslexic and control children is measured in a different study using the cross-approximate entropy (ApEn) methodology. The findings point to positive outcomes for the identification of dyslexic cases (Andreadis et al., 2009). Finding the features that distinguish dyslexic patients before and after treatment is the goal of another study. BrainWare SAFARI software is used for occupational therapy and transcranial direct current stimulation as part of the treatment. Before and after treatment, sixteen dyslexic children's EEG signals are obtained. The most discriminative subset had an accuracy of 92% with the SVM classifier, indicating significant changes in EEG features (Oliaee et al., 2022).

This study examined the changes in brain connectivity patterns in children with developmental dyslexia after they underwent a specific training session. EEG data are recorded from 14 participants diagnosed with dyslexia, at two time points: Day 1 (baseline) and Day 60 (post-training). In order to measure the functional relationships between different regions of the brain, we retrieved a large number of connectivity variables from the EEG. Magnitude squared coherence (MSC), cross-power spectral density (CPSD), covariance (Cov), Pearson correlation coefficient (PC), and entropy-based metrics (correntropy coefficient (RE_Coef), cohentropy coefficient (CE_Coef)) are among them. These diverse measures allowed us to capture both linear (e.g., Coef, Cov, MSC) and nonlinear (e.g., CE_Coef, RE_Coef) interactions, providing a comprehensive representation of functional brain connectivity in dyslexia. A key contribution of our study lies in the comprehensive computation and application of seven graph-theoretical network metrics, which are used to characterize the topological properties of the functional brain networks. Although such metrics have been employed in various EEG studies, their combined use across multiple connectivity measures in a longitudinal dyslexia study is a novel contribution. These metrics include: assortativity, transitivity, clustering coefficient, global efficiency, local efficiency, modularity, and characteristic path length. By analyzing these metrics across two time points, we aimed to capture the dynamic reorganization of brain networks and assess whether the training protocol induced measurable neuroplastic changes in children with dyslexia. All signal processing, feature extraction, and network analysis steps are performed using MATLAB R2025a, a widely used platform for biomedical data analysis and machine learning.

The contributions of this study are as follows:

1. By using a longitudinal, within-subject design to quantify brain network reorganization before (Day 1) objectively and after (Day 60) intervention, our study focuses on tracking neuroplasticity in contrast to the majority of the literature, which focuses on diagnosing dyslexia (comparing patient vs. control groups).
2. In order to create objective, high-temporal resolution biomarkers for evaluating the effectiveness of cognitive training—a critical step for clinical application—we will emphasize the novelty of integrating cutting-edge techniques—EEG-derived functional connectivity (particularly nonlinear metrics like RE Coef), Graph Theory, and Machine Learning.

2. Materials and Methods

This section presents an outline of the suggested structure for the current investigation. This study evaluated the response of children with dyslexia to specific training sessions based on network metrics calculated from the EEG signal. In Figure 1, the system's overall flowchart is shown. A more thorough discussion of the methods will be covered later in this section.

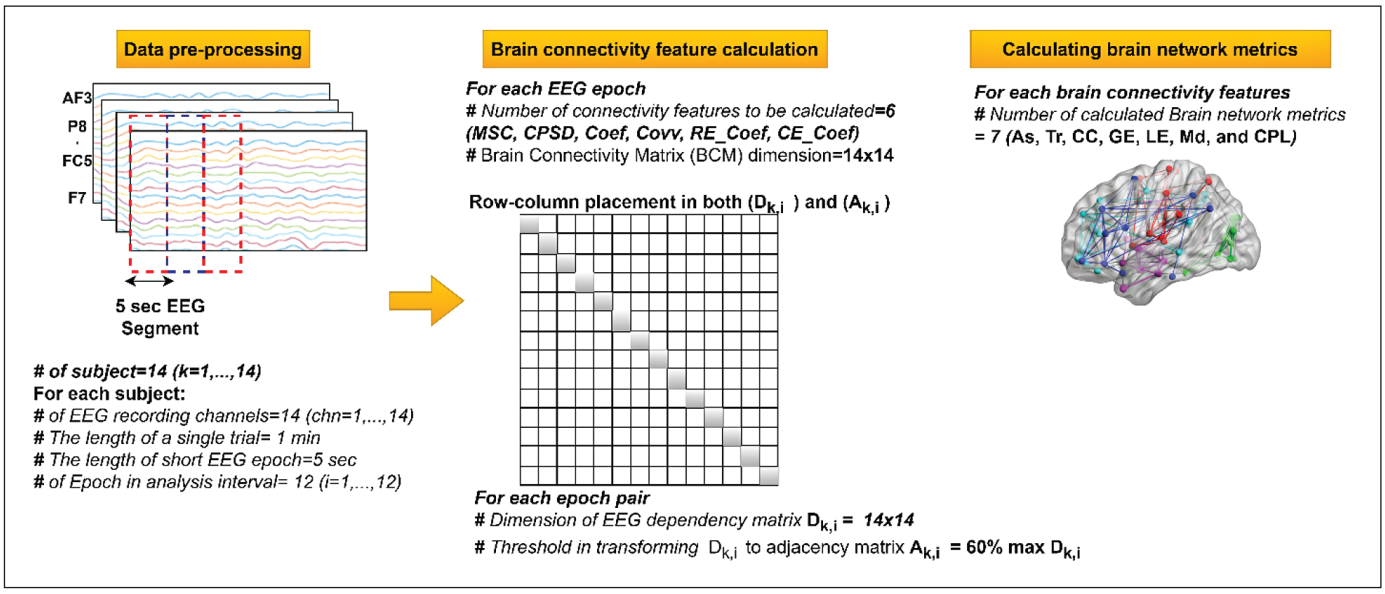

Figure 1. The main steps of the EEG analysis procedure.

2.1. The Participants, Clinical Evaluation, and EEG Data Collection

This study utilizes data from 14 children with pure dyslexia from a clinical intervention that investigated the positive effects of the Auto Train Brain (Eroglu et al., 2022; Eroğlu & Arman, 2023). Following the rules established by the study ethics committee, all participants gave their informed consent before the experiment after being fully informed about the experimental technique. THE EMOTIV EPOC-X Headset is used during the investigations. Each subject received thirty minutes of visual and auditory neurofeedback, six months of Auto Train use, and brain wave measurements across fourteen channels utilizing the EMOTIV EPOC-X. The 1-minute resting-state eyes-open EEG readings are acquired before every neurofeedback session.

We evaluated spontaneous EEG data collected before neurofeedback sessions on Day 1 (the first day) and Day 60 (the sixty-first day) of the Auto Train Brain system, which is utilized by 14 dyslexic children in this study. Recordings are made using a 14-channel EEG system with electrodes placed according to the international 10–20 system. The electrode positions included AF3, AF4, F7, F3, FC5, T7, P7, O1, O2, P8, T8, FC6, F4, and F8. Signals are recorded at a sampling rate of 500 Hz. The ground electrode is located at FPz, and the reference is placed on the left mastoid. Recordings are performed in a quiet room with minimal external distractions. Each session consisted of a single 1-minute trial recorded with the subject in a relaxed, eyes-open state.

2.2. EEG Preprocessing

EEG preprocessing is conducted using MATLAB R2025a and the EEGLAB toolbox. Raw EEG signals are band-pass filtered between 0.5 Hz and 45 Hz to remove slow drifts and high-frequency noise, preserving neural activity relevant to cognitive processing, including delta, theta, alpha, beta, and low gamma frequency bands. Artifact components such as eye blinks and muscle activity are removed using Independent Component Analysis (ICA). The continuous 1-minute EEG recordings are segmented into 12 non-overlapping 5-second epochs. Epochs exhibiting voltage fluctuations exceeding ±100 μV are rejected. Baseline correction is applied to all remaining epochs before further analysis.

2.3. Functional Connectivity-Based Feature Extraction

To capture inter-regional communication, six different pairwise connectivity measures are calculated between all possible electrode pairs for each 5-second epoch. These measures included: MSC, CPSD, PC, Cov, RE_Coef, and CE_Coef. These features are selected to capture both linear (e.g., PC, MSC, Cov) and nonlinear (e.g., RE_Coef, CE_Coef) dependencies among brain regions. Feature values are computed for each epoch.

2.3.1. Cross-Power Spectral Density

CPSD is used in the frequency domain to examine the cross-correlation between two time series. The cross-spectral density describes how the covariance between two sets of data is distributed over the frequency range (Li et al., 2020). Given two EEG channel epochs (and) as random variables, the following formula defines CPSD:

$$P_{x,y}(\omega) = \sum_{k=-\infty}^{\infty} R_{x,y}(k) e^{-j\omega k} \quad (1)$$

The cross-correlation between two signals, X and Y, is indicated by $R_{x,y}$ (k), and the CPSD, which is a complex function determined by the discrete-time Fourier transform of the cross-correlation, is indicated by $P_{x,y}(\omega)$. The CPSD, $CPSD(\omega)=\frac{1}{n} \mid P_{x,y}(\omega)|^2$, is computed using the Welch estimation. For uncorrelated signals, the CPSD is zero at all frequencies (Li et al., 2020).

2.3.2. Magnitude-Squared Coherence

MSC is a frequency-domain metric used to quantify the linear relationship between two signals, such as EEG time series, across specific frequency bands. In neuroscience, MSC is widely employed to evaluate the strength and stability of functional connectivity between cortical regions, particularly in cognitive domains such as attention, perception, and language. A high MSC value indicates strong synchronization between brain regions, suggesting coordinated neural activity. To improve reliability, MSC is typically calculated using Welch's method, which averages spectral estimates over overlapping data segments (Suhail et al., 2022). Formally, Equation 2, which gives the MSC between two random variables X and Y.

$$MSC_{x,y}(\omega) = \frac{|P_{x,y}(\omega)|^2}{P_{x,x}(\omega) P_{y,y}(\omega)} \quad (2)$$

The power spectral densities of X and Y, respectively, are represented by the symbols $P_{x,x}(\omega)$ and $P_{y,y}(\omega)$, which are determined by the discrete-time Fourier transforms of the auto-correlation sequences $R_{x,x}(\omega)$ and $R_{y,y}(\omega)$. $R_{x,y}(\omega)$ is used to determine the cross power spectral density of X and Y, which is represented by $P_{x,y}(\omega)$. MSC assigns a number to each frequency that ranges from 0 to 1. A perfect linear connection between two signals is denoted by a value of 1, whereas a value of 0 denotes linear independence.

2.3.3. Covariance and Pearson Correlation Coefficient

The covariance matrix provides information on how many random variables are correlated. Details about the relationship between EEG signals recorded at various electrode sites over time are provided by the covariance matrix. Determining the changes in the relative activity of various brain regions depends on this information (Jiang et al., 2019; Aydin et al., 2022). Cov offers a linear statistical measure to assess linear dependency between two EEG recording sites in the form, given two EEG segments (X and Y) as random variables with mean values (μ_x, μ_y).

$$Cov_{x,y} = \frac{1}{N} \sum_{k=1}^{N} (x_k - \mu_x)(y_k - \mu_y)$$
$$PC_{xy} = \frac{1}{N} \sum_{k=1}^{N} \frac{(x_k - \mu_x)(y_k - \mu_y)}{\sigma_x \sigma_y} \quad (3)$$

The PC is a statistical measure that quantifies the linear relationship between two EEG channel signals by normalizing their covariance by the product of their standard deviations (σ_x and σ_y)

$$PC_{x,y} = \frac{Cov_{x,y}}{\sigma_x \sigma_y} \quad (4)$$

In the context of functional connectivity analysis, PC assesses how amplitude fluctuations in one channel align with those in another over time, providing a value between −1 (perfect negative correlation) and +1 (perfect positive correlation) (Šverko et al., 2022; Aydin et al., 2022).

2.3.4. Correntropy Coefficient and Cohentropy Coefficient

The RE_Coef is a nonlinear similarity measure designed for multichannel signal analysis, particularly effective in capturing both second-order and higher-order statistical dependencies. An extension of the correlation coefficient that finds higher-order statistical or nonlinear correlation between signals is the correntropy coefficient. The centered cross-correntropy $C_{x,y}$, which is a generalization of covariance, is normalized. By making signals dimensionless, normalization enables various dynamics.

$$C_{x,y} = \frac{1}{N} \sum_{k=0}^{N-1} K(x_k, y_k) - \frac{1}{N^2} \sum_{k,l}^{N-1} K(x_k, y_l) \quad (5)$$

In this case, K(.) is a symmetric positive definite kernel function, and N is the number of samples.

$$RE\_Coef = \frac{C_{x,y}}{\sqrt{C_{x,x}}\sqrt{C_{y,y}}} \quad (6)$$

where the kernel has a major impact and RE_Coef stands for the correntropy coefficient. The boundaries of the RE_Coef are -1 and 1. The RE_Coef will be zero if the two signals are independent. RE_Coef tends toward -1 when two variables are related in opposite directions, and it approaches 1 when they are dependent in the same direction (Dauwels et al., 2010; Gunduz & Principe, 2009; Xu et al., 2008).

The CE_Coef is a nonlinear similarity measure derived by extending the correntropy concept to the frequency domain, aiming to capture higher-order statistical dependencies between signals beyond linear coherence. It operates by computing kernel-based similarities between the Fourier-transformed, normalized versions of two signals, thus allowing for the detection of complex interactions in the spectral domain that traditional coherence may overlook. This approach enhances sensitivity to nonlinear and phase-invariant relationships in EEG connectivity analysis (Dauwels et al., 2010; Gunduz & Principe, 2009) and formulation is given in Equation 7;

$$CE\_Coef = \frac{\langle K(X(\omega),Y(\omega))\rangle}{\sqrt{\langle K(X(\omega),X(\omega))\rangle}\sqrt{\langle K(Y(\omega),Y(\omega))\rangle}} \quad (7)$$

where ⟨.⟩represents the average. Fourier transformations of the signals (X(ω) and Y(ω)) must be normalized by the mean and standard deviation prior to calculating the cohentropy coefficient.

Using the above calculated connectivity-based metrics, a 14X14 brain connectivity matrix (BCM) is generated for each epoch. BCM will be defined as follows:

$$BCM = \begin{bmatrix} w_{11} & w_{12} & \cdots & w_{1n} \\ w_{21} & w_{22} & & w_{2n} \\ \vdots & & \ddots & \vdots \\ w_{n1} & w_{n2} & \cdots & w_{nn} \end{bmatrix} \in R^{14X14XN_z} \quad (8)$$

In this case, n is the EEG epoch number, and w_{ij} is the connectivity-based feature value that is determined for each EEG segment between the i and j EEG channel pairings. By arranging these w_{ij} values in a 14x14 matrix, "BCM"—a brain connection matrix with 14 nodes—will be produced. This connectivity matrix is then defined as the dependency matrix ($D_{k,i}$), and a specific thresholding process is applied to obtain the adjacency matrix ($A_{k,i}$). The threshold value is set at 60% of the maximum value in each dependency matrix.

2.4. Network Analysis Based on Graph Theory

In this study, graph theoretical analysis is applied to EEG-derived functional connectivity networks across Day 1 and Day 60. Functional connectivity matrices are constructed per subject using multiple estimators. To ensure connected and meaningful network structures, proportional thresholding retaining 60% of the strongest connections is applied. An initial trial-and-error analysis is used to determine this range. The results indicated that a 60% sparsity threshold is the most appropriate value that simultaneously guaranteed full network connectivity across all 14 subjects and eliminated weak, potentially spurious connections, thereby representing a biologically meaningful core network. We discovered that although higher sparsity (e.g., 90%) faced the risk of retaining excessive noise, lesser sparsity (e.g., 50%) faced the danger of losing connectivity.

Each thresholded adjacency matrix is represented as an undirected weighted graph. Seven graph metrics are computed for each network: assortativity, transitivity, clustering coefficient, global efficiency, local efficiency, modularity, and characteristic path length. These metrics are calculated across connectivity methods, producing a feature set of 7 metrics x 6 connectivity-based features = 42 features.

2.4.1. Assortativity

The likelihood of nodes in a network linking with other nodes that share a similar characteristic is measured by assortativity (As). In functional brain networks, node degree is typically used to calculate it. The robustness and modularity of networks can be improved by positive assortativity, which shows that nodes with high degrees have a tendency to connect to other high-degree nodes. A reduction in assortativity has been noted in certain brain illnesses, and negative assortativity suggests linkages between high-degree and low-degree nodes (Aydin et al., 2022; Chen et al., 2019; Newman, 2002).

2.4.2. Transitivity

The ratio of triangles in the network, or the probability that a node's neighbors are likewise connected, is expressed by transitivity (Tr). High transitivity in functional brain networks reflects coordinated activity and local information

processing capacity by indicating substantial local clustering and modular structure (Aydin et al., 2022; Chen et al., 2019; Rubinov & Sporns, 2010).

2.4.3. Clustering Coefficient

The ratio of the connections that currently exist between a node's neighbors to the maximum number of connections that may exist is known as the clustering coefficient (CC). This measure shows that there are functional modules in the brain and represents the density of local connections. It is typical to find high clustering coefficients in small-world networks (Aydin et al., 2022; Chen et al., 2019).

2.4.4. Global Efficiency

Global efficiency (GE) is defined as the inverse of the average shortest path length between all pairs of nodes in the network. This metric indicates how efficiently information is exchanged across the entire network. High global efficiency in brain networks reflects strong integrative processing capacity and effective communication (Aydin et al., 2022; Chen et al., 2019; Latora & Marchiori, 2001).

2.4.5. Local Efficiency

Local efficiency (LE) quantifies the effectiveness of information sharing among a node's neighbors after that node is eliminated. It stands for both the local processing efficiency and the network's fault tolerance. Local communication efficiency within local clusters or modules is referred to as local efficiency in brain networks (Chen et al., 2019; Latora & Marchiori, 2001).

2.4.6. Modularity

In order to maximize the number of within-group edges and reduce the number of between-group edges, the network should be divided into nonoverlapping groups of nodes. This is the ideal community structure. One metric that measures how easily the network can be separated into such distinct groups is called modularity (Md) (Aydin et al., 2022; Chen et al., 2019).

2.4.7. Characteristic Path Length

The network characteristic path length (CPL) is the average shortest path length between all pairs of nodes in the network. The global efficiency is the average inverse shortest path length in the network. The nodal eccentricity is the maximal path length between a node and any other node in the network. The radius is the minimal eccentricity, and the diameter is the maximal eccentricity (Chen et al., 2019; Rubinov & Sporns, 2010).

2.5. Classification and Performance Evaluation

To evaluate whether changes in brain connectivity and network topology could effectively discriminate between Day 1 and Day 60, supervised machine learning algorithms are employed using a comprehensive feature set. All extracted graph measures—seven metrics calculated across six connectivity features, yielding 42 features—are included in the input dataset. The classification algorithms applied included Decision Tree (DT), Logistic Regression (LR), k-Nearest Neighbors (kNN), Support Vector Machine (SVM), and Bagged Trees (BT).

2.5.1. Decision Tree

A decision tree is a non-parametric learning technique for regression and classification that uses data features to learn basic decision rules that predict the value or class of a target set of data. Every node works with a feature, and leaves examine class labels according to the value of the feature (Tor et al. 2021; Zaree et al. 2023). The "Fine DT" technique is used in our simulation, which allows the tree to grow to its maximum depth by requiring a minimum leaf size of 1.

2.5.2. Logistic Regression

A statistical model that uses the logistic function for binary classification problems is called Binary Logistic Regression. Because of its great interpretability and robustness, it is useful in biomedical and clinical research where it is essential to comprehend the impact of individual predictors. It is a member of the family of generalized linear models (Zingoni et al., 2024). The standard defaults, which usually incorporate L2 regularization (Ridge) with a regularization strength of C=1.0, are employed by LR in our simulations.

2.5.3. k-Nearest Neighbors

A non-parametric, instance-based learning technique called the k-Nearest Neighbors (kNN) algorithm categorizes a data point according to the majority class of its k nearest neighbors in feature space. A modest number for k (such as k=1 or k=3) is commonly used in "fine" KNN models, which produce extremely sensitive and detailed decision boundaries. Although it can be computationally costly and sensitive to noisy features, it is straightforward and efficient, especially for datasets with nonlinear class borders (Anuragi et al., 2022; Tor et al., 2021; Zaree et al., 2023). In our simulation, "Fine kNN" is used by utilizing euclidean distance metric, uniform weighting and k=3.

2.5.4. Support Vector Machine

A supervised learning model linked to learning algorithms used in machine learning for classification is the support-vector machine (SVM). Using the kernel method, which implicitly transfers the input data into a high-dimensional feature space, SVMs are capable of both linear and effective non-linear classification. The linear kernel is used in our study because it simplifies the model and reduces computation time while achieving high classification performance in many applications (Gallego-Molina et al., 2022; Parmar & Paunwala, 2023; Tor et al., 2021; Zaree et al., 2023). In order to balance margin maximization with classification error, we used SVM in our simulation using a linear kernel and the default regularization parameter of C=1.0.

2.5.5. Bagged Trees

By employing numerous learning algorithms, the ensemble approach improves the classifier's performance and lessens over-fitting. Bagging is a popular ensemble technique that decreases the large variance of the algorithm, like a decision tree, making it more accurate and effective than boosting and random forest (Anuragi et al., 2022; Tor et al., 2021). BT used 100 estimators (base learners) for ensemble methods in our simulation, which is a typical setting for variance reduction.

2.6. Performance Evaluation

Following statistical analysis, model training and validation are rigorously performed through 5-fold cross-validation implemented in MATLAB's Classification Learner Tool, ensuring unbiased estimation of generalization performance. Classification metrics extracted from the tool included accuracy (ACC), sensitivity (SEN), specificity (SPE), and positive predictive value (PPV). Subsequently, the F1-score (F1-S) is computed as the harmonic mean of precision and sensitivity, providing a balanced measure that reflects the trade-off between type I and type II errors—particularly important for neural data with potentially skewed class distributions.

3. Experimental Results and Discussion

The efficiency of the Auto Train Brain system is demonstrated by examining a two-class classification schema to discriminate surface EEG readings taken before neurofeedback sessions on Day 1 (the first day) and Day 60 (the sixty-first day). Using a 14-channel EEG dataset lasting one minute, seven distinct functional connectivity-based features (CPSD, MSC, PC, Cov, RE_Coef, and CE_Coef) are computed for pairs of brief segments. Twelve brain connectivity matrices are acquired for every person since identical segments has a length of 5 seconds. Therefore, for each brain network measure (As, Tr, CC, GE, LE, Md, and CPL), which is calculated for each brain connectivity matrix, there are 168 features ((#of subject) X (# of segments) = 14 X12) in each group. This increases the number of features to seven times 168 when all measurements are taken into account in classifications. Gun1 and Gun60 have the labels 0 and 1, respectively. The performance of several classifiers is investigated using MATLAB 2025Ra's Statistical and Machine Learning toolbox.

In Table 1, the performance evaluation results of classifiers are provided with respect to ACC, SEN, SPE, PPV, and F1-S. An important factor influencing the models' performance is the brain network metric selection. When trained on data obtained from PC and RE_Coef measures, almost all models achieve extraordinarily high scores (typically 100% in ACC, SEN, SPE, PPV, and F1), suggesting that these metrics are the most effective for classification. MSC produces outstanding results as well; the LR and BT models both obtain a flawless 100% F1-S. For the classification models, CPSD and Cov measurements are more difficult. With these metrics, the F1-S for the majority of models significantly decrease. Specifically, the SVM model performs poorly on these, with an F1-S of 97.99% for Cov and 93.10% for CPSD. Additionally, the accuracy and F1-S of the kNN model for CPSD and Cov significantly decline. The table shows that PC, RE_Coef, and MSC are three brain connectivity measures that are very predictive and enable many models to complete classifications almost flawlessly. However, the models have a harder time learning from the CPSD and Cov metrics, which leads to poorer performance, particularly for the kNN and SVM models. In terms of classifying brain network metrics, the BT and LR models are the most dependable and successful, whereas the DT and SVM models are less strong. Overall, this study highlights the critical importance of both algorithm selection and feature engineering for achieving optimal predictive performance in EEG-based diagnostic systems.

In the following, a thorough study is performed using RE_Coef since it produced better findings than other brain connectivity metrics. Based on the RE_Coef measure, Figure 2 shows a comparison of brain connectivity data for two distinct days: Day 1 and Day 60. The connectivities between different brain areas (electrodes) are displayed using

Table 1. Classifier performance results for brain network metrics estimated utilizing CPSD, MSC, PC, Cov, RE_Coef, and CE_Coef.

		ACC	SEN	SPE	PPV	F1-S
CPSD	**DT**	99.25	99.04	99.64	99.70	99.37
	LR	97.68	96.79	98.39	99.23	97.94
	SVM	91.63	92.09	89.53	94.30	93.10
	kNN	88.41	89.79	84.99	91.19	90.36
	BT	98.94	98.51	99.64	99.69	99.09
MSC	**DT**	98.38	98.21	98.66	99.20	98.69
	LR	100.00	100.00	100.00	100.00	100.00
	SVM	99.52	99.22	100.00	100.00	99.60
	kNN	98.31	99.03	97.01	98.26	98.62
	BT	98.88	98.72	99.12	99.48	99.09
PC	**DT**	100.00	100.00	100.00	100.00	100.00
	LR	99.61	99.58	99.68	99.76	99.67
	SVM	99.73	99.84	99.66	99.77	99.80
	kNN	98.13	99.59	95.89	97.51	98.52
	BT	99.86	99.79	100.00	100.00	99.89
Cov	**DT**	99.87	99.84	100.00	100.00	99.92
	LR	98.30	98.14	98.39	99.11	98.61
	SVM	97.44	97.30	96.92	98.81	97.99
	kNN	91.86	92.54	90.26	94.25	93.34
	BT	99.87	99.84	100.00	100.00	99.92
CE_Coef	**DT**	100.00	100.00	100.00	100.00	100.00
	LR	99.58	99.56	99.60	99.41	99.48
	SVM	99.86	99.79	100.00	99.60	99.70
	kNN	96.29	96.67	95.47	97.19	96.88
	BT	100.00	100.00	100.00	100.00	100.00
RE_Coef	**DT**	99.48	99.15	100.00	100.00	99.56
	LR	99.85	99.78	100.00	100.00	99.89
	SVM	99.85	99.78	100.00	100.00	99.89
	kNN	99.09	99.01	99.28	99.49	99.24
	BT	99.32	98.89	100.00	100.00	99.44

two different kinds of visualizations. The brain connectivity matrices for Day 1 and Day 60 are shown as heatmaps in Figure 2 (a) and (b), respectively. The connectivity's strength is indicated by the color scale, which ranges from deep blue (low connectivity) to blazing red (high connectivity). connectivities are poor and appear blue and green on Day 1. On Day 60, there is an increase in connections, with the colors yellow, orange, and red signifying a greater degree of interconnectedness between different parts of the brain. This implies that this rise might have been influenced by training, learning, or modifications in cognitive state.

The connectivity that exceeded the 60% threshold are shown in Figure 2 (c) and (d), which are circular connectivity graphs that offer an alternate, aesthetically pleasing depiction of the same data. A common technique for visualizing networks, especially in neuroscience, is the circular layout, which uses

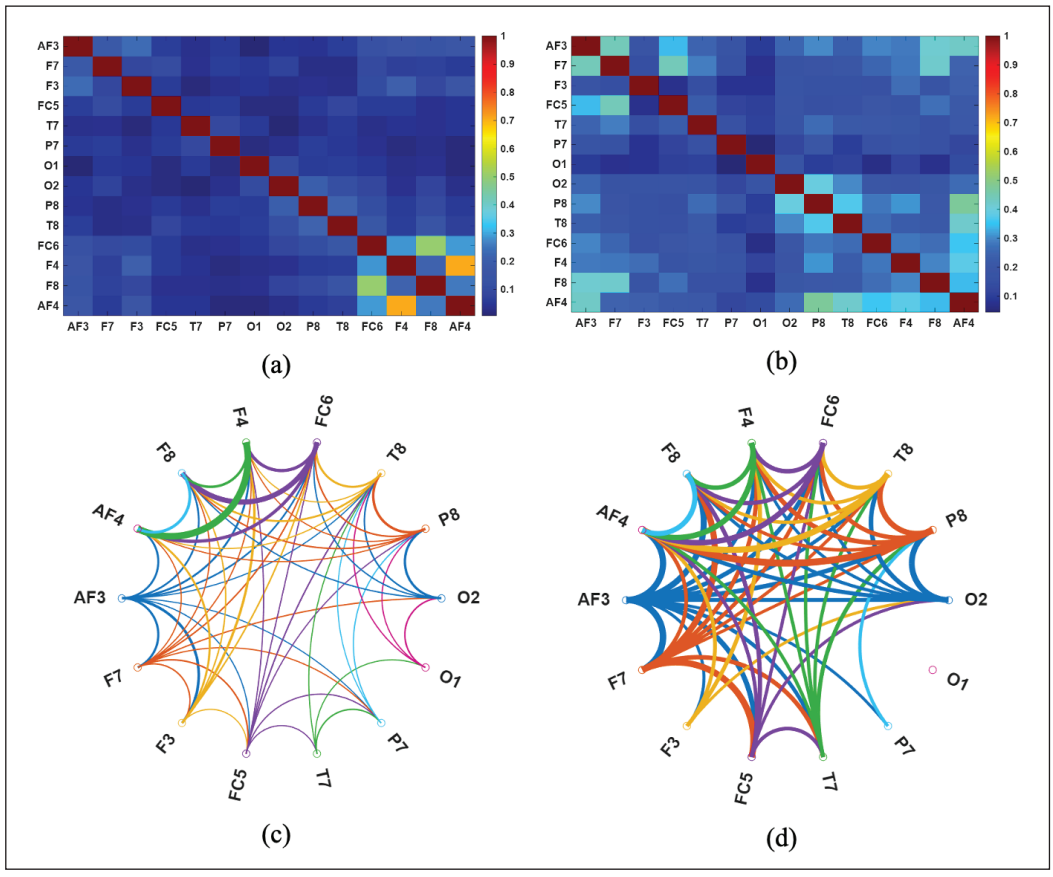

Figure 2. (a) Brain connectivity matrix, (c) circular connectivity graph obtained with 60% threshold value of RE_Coef for Day 1; (b) Brain connectivity matrix, (d) circular connectivity graph obtained with 60% threshold value of RE_Coef for Day 60.

curved lines and nodes to give an obvious overview of the network's structure. The nodes in the graph are color-coded to represent various groups or modules and are labeled with brain channel or region identifiers. The thickness and color of the edges indicate the strength of the functional connections between different parts of the brain. The RE_Coef metric, which measures variations in brain activity patterns across several areas, serves as the basis for the graph. Comparing the Day 60 graph (Figure 2 (d)) to the Day 1 graph (Figure 2 (c)), it is evident that the connecting lines are thicker and appear more intense. This shows that during the 60 days, the functional connections between different brain regions (such as frontal–occipital and temporal–parietal) have either gotten stronger or become more noticeable. Notwithstanding their similar structure, the "Day 60" graph indicates greater interaction between functional groupings or brain lobes due to its more dominant pathways and thicker connections. The brain's functional network shows a notable shift from "Day 1" to "Day 60," with stronger connections and an increase in thickness and density over a period of 60 days. In general, sparse connectivity on Day 1 suggests a modular network structure. Stronger connection on Day 60 suggests a denser, more integrated network with substantial inter-regional brain interaction. The functional brain network is reorganized from localized specialization to global integration over the transition from Day 1 to Day 60, which may increase connectedness but decrease efficiency.

The most significant measurements that are responsive to cognitive training are highlighted by applying the one-way ANOVA test at the subject level to determine statistical differences between groups in terms of statistical factors in brain network metrics computed using RE_Coef. The one-way ANOVA test is performed (at α=0.05) to determine if there are statistically significant differences in brain network metrics—derived using RE_Coef—across the defined groups. One-way ANOVA is used for the statistical analysis at the subject level. For RE_Coef connectivity-based feature of each subject in each session (Day 1 and Day 60), the mean of the seven graph theory features is calculated over all valid EEG epochs (≅12). These subject-averaged features are then subjected to an ANOVA to specifically test for the main impact of the training process. Table 2 lists the com-

Table 2. Group-to-group statistical test results for brain network measures derived from RE_Coef (in one-way Anova tests, SS: Sum of squares due to each source, MS: Mean squares for each source (the ratio between SS and the degree of freedom), F: F-statistic (the ratio of the mean quare), Prob > F: p-values).

	One-way ANOVA test			
	SS	MS	F	Prob>F
As	0.5692	0.5692	25.86	1.00E-04
Tr	0.1260	0.1260	27.56	5.10E-07
CC	0.1218	0.1218	34.70	4.42E-08
GE	0.1044	0.1044	41.58	2.23E-09
LE	0.1471	0.1471	39.30	6.15E-09
Md	0.0176	0.0176	4.83	2.10E-01
CPL	12492.9	12492.9	2003.7	9.54E-178

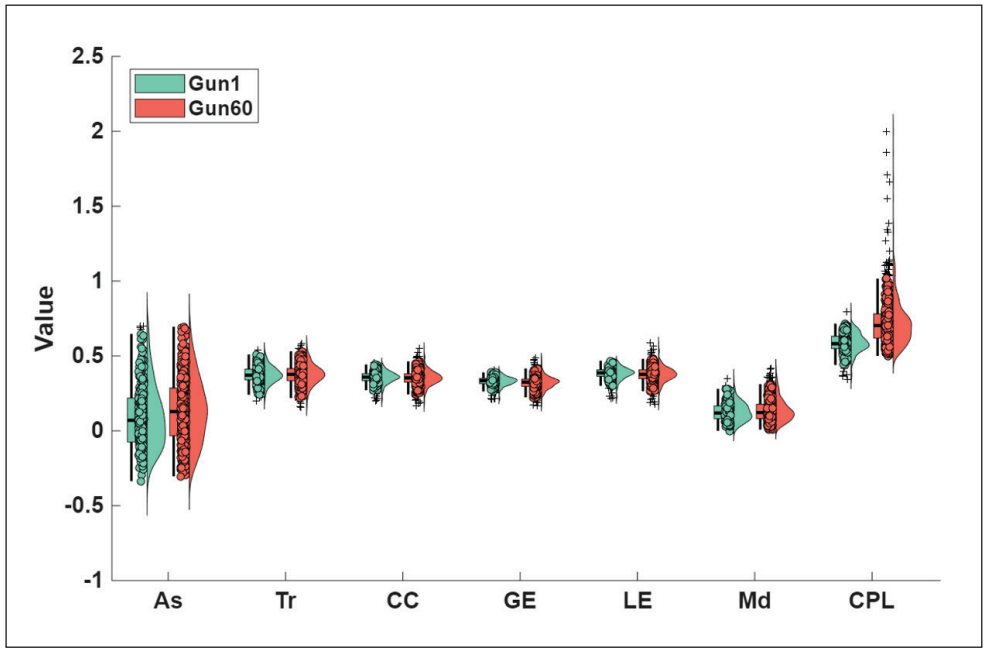

Figure 3. The violin plot representation of brain network metrics that are calculated using a RE_Coef.

parable outcomes. Notably, all six indices (As, Ts, CC, GE, LE, and CPL) produced significant and substantial statistical differences with low p-values ($p<0.05$), with the exception of the modularity indicator, Md.

Along with thorough statistical analyses and classification procedures, Figure 3 also displays violin plots of brain network metrics that are calculated using a RE_Coef. The distributions of several metrics on Day 1 (green violins) and Day 60 (orange) are compared. Minimal differences between groups are seen in Tr, CC, GE, and LE, indicating that fundamental small-world characteristics are mostly unchanged. This indicates that the network's basic small-world characteristics, such as its propensity to form clusters and retain efficiency, are maintained even as it becomes denser. As for "As", Gun1 exhibits a more constrained distribution with a center close to zero, but Gun60 displays a wider range that includes both negative and higher positive values. At Day 60, there is a greater fluctuation. A decrease in Md is indicated by Gun60 shifting slightly downward and Gun1 values clustering around positive values. At day 60, Md declines, which is consistent with the circular connectivity graph's observation of the disappearance of distinct communities. There is an obvious difference between the CPL of Gun60 and Gun1; Gun60 has larger values and a higher spread. The findings of visual connectivity (seen in Figure 2) are supported by network metrics. Day 60 demonstrates more robust connections overall, but at the expense of modularity and efficiency. From Day 1 to Day 60, the

network reorganizes from segregated, modular, and efficient brain networks to denser, globally interconnected networks, which results in reduced efficiency (Figures 2 and 3). Increased global connectivity in the brain could be a sign of a compensatory reorganization process that results in a decrease in optimal network organization, which could suggest network adaptability or degeneration.

Sophisticated models and benchmarking studies have proliferated in recent years. The performance of the suggested system is contrasted with earlier research that was published in the literature to make benchmarking easier, as shown in Table 3. The proposed method, which combines EEG-based functional connectivity, graph theoretical analysis, and machine learning, is remarkably successful at capturing training-induced neuroplastic changes, as the classification results show. For the best-performing metrics (RE_Coef, MSC), our reported range of Accuracy (ACC: 88.41%–100%) and Sensitivity (SEN: 89.79%–100%) is extremely competitive and approaches the highest success rates in the literature (e.g., Christodoulides et al., 2022; Parmar & Paunwala, 2023; Seshadri et al., 2023). The best metric, RE_Coef, achieved almost flawless classification (ACC ~100% with a narrow distribution), demonstrating that a highly separable feature space is created by the dynamic changes in brain network architecture between Day 1 and Day 60. The use of these combined features as reliable and measurable biomarkers for monitoring the results of cognitive treatment is validated by this high performance. Our work fills a crucial gap in dyslexia research with sevreral important features

Table 3. Performance comparison of the suggested model with relevant earlier research in automated dyslexia identification.

Reference	Subject	Method	Results
Andreadis et al., 2009	38 Dyslexia 19 Control	Cross Approximate Entropy	ACC=78.95% SEN=89.47% SPE=57.89%
Castillo-Barnes et al., 2024	15 Dyslexia 33 Control	Cross-Frequency Coupling	ACC=79.09% AUC=82.1%
Christodoulides et al., 2022	12 Dyslexia 14 Control	Spectral features extracted from each EEG rhythm	ACC=98.01% SEN=98.73% SPE=97.39 %
Christoforou et al., 2021	30 Dyslexia 30 Control	Rapid-Automatized Naming (RAN) task	Not given
Gallego-Molina et al., 2022	16 Dyslexia 32 Control	Phase-Amplitude Coupling and Complex Network Analysis	ACC=72.9% SEN=72.3% SPE=74.7% AUC=73.3%
Oliaee et al., 2022	15 Dyslexia	Spectral features Harmonic features Phase-related features EMD-based features	ACC=92%
Parmar & Paunwala, 2023	195 Dyslexia 196 Control	Wavelet Scattering Transform	ACC=96.96%~97.12%
Seshadri et al., 2023	15 Dyslexia 15 Control	Functional brain networks	ACC=96.7% SEN=93% SPE=100% AUC=96%
Zaree et al., 2023	22 Dyslexia 22 Control	Evoked-related potentials during a Visual Continuous Performance Task	ACC=87.5% SEN=81.2% SPE=93.7%
Proposed study	**14 Dyslexia Before and after cognitive training**	**Functional connectivity and Network Analysis**	**ACC=88.41%~100% SEN=89.79%~100% SPE=84.99%~100%**

that set it apart from the high-performing approaches in the comparative literature (Table 3): (i) In contrast to most of the research in this table (which concentrates on diagnosing dyslexia by categorizing dyslexia vs. control individuals), our study specifically examines the brain's ability to heal and adapt by classifying before vs. after cognitive training within the dyslexia group. Therefore, compared to research that focuses on differentiating between the EEG signals of two different groups, this job is more difficult. The requirement for objective indicators of therapy efficacy is immediately addressed by this. (ii) The improved performance of nonlinear connectivity metrics (RE_Coef and CE_Coef) is highlighted in our study. While techniques such as wavelet scattering (Parmar & Paunwala, 2023) and spectral features (Christodoulides et al., 2022) achieve high accuracy, our findings indicate that metrics sensitive to complex, non-linear synchronization and higher-order statistical dependencies best capture the neuroplastic reorganization process. (iii) We go beyond mere connectivity strength by using seven graph theory metrics (GE, LE, CC, etc.). Compared to straightforward feature-based classification, this enables us to measure changes in the network's organizational structure and communication efficiency, which is more indicative of complex cognitive operations.

4. Conclusion and Suggestions

This study demonstrates that EEG-based functional connectivity analysis, combined with graph theory metrics, can effectively capture and quantify neuroplastic changes in children with developmental dyslexia following a structured 60-day cognitive training program. The results revealed substantial improvements in brain network integration, organization, and long-range connectivity, particularly in measures derived from the RE_Coef and PC features, which consistently outperformed other metrics across multiple machine learning algorithms. Binary GLM Logistic Regression achieved the most balanced performance, with accuracy, sensitivity, and specificity exceeding 97% for all features, while Fine KNN and Linear SVM also yielded high accuracy, especially with RE_Coef, though their performance declined for CPSD and Cov. This variation underscores the importance of selecting highly informative features when developing EEG-based diagnostic or monitoring tools. Circular connectivity graphs further illustrated the neural reorganization process, showing a shift from less organized and asymmetric patterns at baseline to more symmetrical, efficient, and long-distance connections after training, with stronger inter-hemispheric links suggesting enhanced coordination between hemispheres relevant to language and reading processes.

The graph theory analysis, encompassing seven critical metrics—assortativity, transitivity, clustering coefficient, global efficiency, local efficiency, modularity, and characteristic path length—provided a multidimensional characterization of topological reorganization. Over time, increases in global and local efficiency indicated improved integration and fault tolerance within brain networks, while transitivity and clustering coefficient increases reflected greater local specialization and redundancy. A notable reduction in characteristic path length over time suggested that the average shortest path between cortical regions decreased, indicating more efficient brain-wide information flow. Modularity values further revealed a refinement in community structures within the brain networks, suggesting that after training, functional modules became more distinct and specialized. This reorganization is a hallmark of healthy network maturation and supports the hypothesis that cognitive training facilitates modular differentiation in dyslexic brains.

These findings not only confirm that targeted cognitive interventions can induce measurable changes in the functional architecture of dyslexic brain networks but also indicate that EEG-based graph metrics, particularly RE_Coef and PC, have strong potential as objective biomarkers for evaluating treatment efficacy. Building on these results, future research should expand participant diversity and sample size to improve generalizability, integrate complementary neuroimaging modalities such as fMRI or MEG to gain a multimodal perspective, and refine feature engineering approaches to enhance the discriminative power of metrics with weaker performance. Additionally, longitudinal follow-up is essential to assess the persistence of training-induced changes, and the development of adaptive, real-time neurofeedback or cognitive training platforms informed by EEG biomarkers could enable personalized interventions tailored to each child's neural profile. Collaboration between neuroscientists, clinicians, and educators would further facilitate the translation of these findings into practical tools for early screening, targeted remediation, and classroom support strategies. Ultimately, the integration of EEG-derived connectivity measures, graph theory analysis, and advanced machine learning holds promise not only for advancing our understanding of the neural basis of dyslexia but also for shaping more effective, individualized, and sustainable intervention programs.

Acknowledgment: We are very appreciative of the families who took part in this study; we might not have finished it without their commitment and encouragement.

Author contribution: All authors contributed equally to the conception, literature review, writing, and revision of the manuscript. All authors have read and approved the final version.

Ethics committee approval: All of the participants provided their informed consent after the research ethics committee explained the experimental procedure to them, the Yeditepe University Ethics Committee approved the study protocol, and the clinical trial was registered with the Türkiye Pharmaceuticals and Medical Devices Agency (TİTÇK) (Nbr: 71146310-511.06,2.11.2018).

Conflict of interest: The authors certify that they have no conflict of interest.

References

Andreadis, I. I., Giannakakis, G. A., Papageorgiou, C., & Nikita, K. S. (2009). Detecting complexity abnormalities in dyslexia measuring approximate entropy of electroencephalographic signals. In 2009 annual international conference of the IEEE engineering in medicine and biology society (pp. 6292-6295). IEEE. https://doi.org/10.1109/IEMBS.2009.5332798

Anuragi, A., Sisodia, D. S., & Pachori, R. B. (2022). EEG-based cross-subject emotion recognition using Fourier-Bessel series expansion based empirical wavelet transform and NCA feature selection method. Information Sciences, 610, 508-524. https://doi.org/10.1016/j.ins.2022.07.121

Aydın, S., Cetin, F. H., Uytun, M. Ç., Babadagi, Z., Gueven, A. S., & Işık, Y. (2022). Comparison of domain specific connectivity metrics for estimation brain network indices in boys with ADHD-C. Biomedical Signal Processing and Control, 76, 103626. https://doi.org/10.1016/j.bspc.2022.103626

Castillo-Barnes, D., Gallego-Molina, N. J., Formoso, M. A., Ortiz, A., Figueiredo, P., & Luque, J. L. (2024). Probabilistic and explainable modeling of Phase–Phase Cross-Frequency Coupling patterns in EEG. Application to dyslexia diagnosis. Biocybernetics and Biomedical Engineering, 44(4), 814-823. https://doi.org/10.1016/j.bbe.2024.09.003

Chen, H., Song, Y., & Li, X. (2019). A deep learning framework for identifying children with ADHD using an EEG-based brain network. Neurocomputing, 356, 83-96. https://doi.org/10.1016/j.neucom.2019.04.058

Christoforou, C., Fella, A., Leppänen, P. H., Georgiou, G. K., & Papadopoulos, T. C. (2021). Fixation-related potentials in naming speed: A combined EEG and eye-tracking study on children with dyslexia. Clinical Neurophysiology, 132(11), 2798-2807. https://doi.org/10.1016/j.clinph.2021.08.013

Christodoulides, P., Miltiadous, A., Tzimourta, K. D., Peschos, D., Ntritsos, G., Zakopoulou, V., ... & Tzallas, A. T. (2022). Classification of EEG signals from young adults with dyslexia combining a Brain Computer Interface device and an Interactive Linguistic Software Tool. Biomedical Signal Processing and Control, 76, 103646. https://doi.org/10.1016/j.bspc.2022.103646

Dauwels, J., Vialatte, F., Musha, T., & Cichocki, A. (2010). A comparative study of synchrony measures for the early diagnosis of Alzheimer's disease based on EEG. NeuroImage, 49(1), 668-693. https://doi.org/10.1016/j.neuroimage.2009.06.056

Eroglu, G., Köprülü, M., & Karabacak, B. (2022). Dyslexia biomarker detection with QEEG data in children: Feasibility, Acceptability, Economic impact, Pilot Study and Survey Results. Qeios, 1-19. https://doi.org/10.32388/4W9RXU.8

Eroğlu, G., & Arman, F. (2023). k-Means clustering by using the calculated Z-scores from QEEG data of children with dyslexia. Applied Neuropsychology: Child, 12(3), 214-220. https://doi.org/10.1080/21622965.2022.2074298

Gallego-Molina, N. J., Ortiz, A., Martínez-Murcia, F. J., Formoso, M. A., & Giménez, A. (2022). Complex network modeling of EEG band coupling in dyslexia: An exploratory analysis of auditory processing and diagnosis. Knowledge-based systems, 240, 108098. https://doi.org/10.1016/j.knosys.2021.108098

Gunduz, A., & Principe, J. C. (2009). Correntropy as a novel measure for nonlinearity tests. Signal Processing, 89(1), 14-23. https://doi.org/10.1016/j.sigpro.2008.07.005

Jiang, D., Yu, M. A., & Yuanyuan, W. A. N. G. (2019). Sleep stage classification using covariance features of multi-channel physiological signals on Riemannian manifolds. Computer Methods and Programs in Biomedicine, 178, 19-30. https://doi.org/10.1016/j.cmpb.2019.06.008

Latora, V., & Marchiori, M. (2001). Efficient behavior of small-world networks. Physical review letters, 87(19), 198701. https://doi.org/10.1103/PhysRevLett.87.198701

Li, H., Feng, S., Ma, L., Xu, Z., Xu, R., & Jung, T. P. (2020). Common cross-spectral patterns of electroencephalography for reliable cognitive task identification. IEEE Access, 8, 17652-17662. https://doi.org/10.1109/ACCESS.2020.2967814

Newman, M. E. (2002). Assortative mixing in networks. Physical review letters, 89(20), 208701. https://doi.org/10.1103/PhysRevLett.89.208701

Oliaee, A., Mohebbi, M., Shirani, S., & Rostami, R. (2022). Extraction of discriminative features from EEG signals of dyslexic children; before and after the treatment. Cognitive Neurodynamics, 16(6), 1249-1259. https://doi.org/10.1007/s11571-022-09794-2

Parmar, S., & Paunwala, C. (2023). A novel and efficient Wavelet Scattering Transform approach for primitive-stage dyslexia-detection using electroencephalogram signals. Healthcare Analytics, 3, 100194. https://doi.org/10.1016/j.health.2023.100194

Peterson, R. L., & Pennington, B. F. (2012). Developmental dyslexia. The lancet, 379(9830), 1997-2007. https://doi.org/10.1016/S01406736(12)60198-6

Rubinov, M., & Sporns, O. measures of brain connectivity: uses and interpretations. NeuroImage 52: 1059-1069. https://doi.org/10.1016/j.neuroimage.2009.10.003

Seshadri, N. G., Singh, B. K., & Pachori, R. B. (2023). EEG based functional brain network analysis and classification of dyslexic children during sustained attention task. IEEE transactions on neural systems and rehabilitation engineering, 31, 4672-4682. https://doi.org/10.1109/TNSRE.2023.3335806

Snowling, M. J., & Hulme, C. (2012). Annual Research Review: The nature and classification of reading disorders–a commentary on proposals for DSM-5. Journal of child psychology and psychiatry, 53(5), 593-607. https://doi.org/10.1111/j.1469-7610.2011.02495.x

Suhail, T. A., Indiradevi, K. P., Suhara, E. M., Poovathinal, S. A., & Ayyappan, A. (2022). Distinguishing cognitive states using electroencephalography local activation and functional connectivity patterns. Biomedical Signal Processing and Control, 77, 103742. https://doi.org/10.1016/j.bspc.2022.103742

Šverko, Z., Vrankić, M., Vlahinić, S., & Rogelj, P. (2022). Complex Pearson correlation coefficient for EEG connectivity analysis. Sensors, 22(4), 1477. https://doi.org/ 10.3390/s22041477

Tor, H. T., Ooi, C. P., Lim-Ashworth, N. S., Wei, J. K. E., Jahmunah, V., Oh, S. L., ... & Fung, D. S. S. (2021). Automated detection of conduct disorder and attention deficit hyperactivity disorder using decomposition and nonlinear techniques with EEG signals. Computer Methods and Programs in Biomedicine, 200, 105941. https://doi.org/10.1016/j.cmpb.2021.105941

Xu, J. W., Bakardjian, H., Cichocki, A., & Principe, J. C. (2008). A new nonlinear similarity measure for multichannel signals. Neural Networks, 21(2-3), 222-231. https://doi.org/10.1016/j.neunet.2007.12.039

Zaree, M., Mohebbi, M., & Rostami, R. (2023). An ensemble-based machine learning technique for dyslexia detection during a visual continuous performance task. Biomedical Signal Processing and Control, 86, 105224. https://doi.org/10.1016/j.bspc.2023.105224

Zingoni, A., Taborri, J., & Calabrò, G. (2024). A machine learning-based classification model to support university students with dyslexia with personalized tools and strategies. Scientific reports, 14(1), 273. https://doi.org/10.1038/s41598-023-50879-7